

## Geochemical tomography for melting condition beneath Japan arcs

NAKAMURA, Hitomi<sup>1\*</sup>, IWAMORI, Hikaru<sup>1</sup>

<sup>1</sup>Tokyo Institute of Technology

Slab-derived fluid (hereafter slab-fluid) plays an important role for generation of arc magmas. If the flux of slab-fluid is enhanced or reduced by variable tectonic settings and the corresponding thermal and flow regimes, it has effects on the mantle melting. The melting condition may contribute to infer the thermal, flow and fluid regimes. We focus on the melting condition in the mantle wedge beneath Central Japan, where the two overlapping slabs, Pacific and Philippine Sea plates, exist and the amount and composition of slab-fluids from the two slabs are well documented, as the regional variation of slab-fluid fluxes that are related to the geometry of the subducting plates.

Based on the chemical composition of major and trace elements, we construct forward and backward models to constrain the melting condition beneath Central Japan. The composition of the primitive rock can be corrected for fractionated phases to estimate backwardly that of primary magma, while the composition of melt generated in the mantle wedge can be forwardly modeled as a function of degree of melting (sensitive to temperature) and mineralogy (proportions of garnet/spinel peridotites, sensitive to pressure) based on the composition of fluid metasomatized mantle.

As a result, the melting condition is characterized by relatively low melting degrees and high proportions of garnet peridotite involved in melting compared to the adjacent arcs with a single subducting slab, e.g., the Izu-arc. This implies that, the melting occurred at deeper depths and lower temperature for Central Japan. This also consistently explains the existence of adakites occurred in this area, in spite of the cold setting. The same analysis for the volcanoes in the adjacent areas show transition the thermal and fluid conditions, according to the spatial variation of the tectonic regimes, suggesting that geochemical approach is useful to map the physical condition, and could be referred to as geochemical tomography.

Keywords: mantle, melting, slab, slab-fluid, subduction, arc

## Experimental constraints on partitioning of hydrogen between plagioclase and basaltic melt

HAMADA, Morihisa<sup>1\*</sup>, USHIODA, Masashi<sup>1</sup>, TAKAHASHI, Eiichi<sup>1</sup>

<sup>1</sup>Department of Earth and Planetary Sciences, Tokyo Institute of Technology

**Introduction:** The hydrogen in nominally anhydrous minerals (NAMs) can be an indicator of H<sub>2</sub>O activity in silicate melts if the partitioning behavior of hydrogen between NAMs and melts is known. Plagioclase is one of the NAMs and one of the most common minerals in arc basaltic rocks. Therefore, hydrogen in volcanic plagioclase (OH) can be a useful proxy of H<sub>2</sub>O in arc basaltic magmas. Here, we report experimental results on the partitioning of hydrogen between Ca-rich plagioclase and basaltic melt. We also apply the OH concentration of plagioclase as hygrometer of melt based on experiments.

**Experimental:** Hydrous melting experiments of arc basaltic magma were carried out at 350 MPa using an internally-heated pressure vessel installed at Magma Factory, Tokyo Institute of Technology. Starting material was hydrous glass (0.8 wt.% <H<sub>2</sub>O<5.5 wt.%) of an undifferentiated rock from Miyakejima volcano, a frontal-arc volcano in Izu-arc (MTL rock: 50.5% SiO<sub>2</sub>, 18.1% Al<sub>2</sub>O<sub>3</sub>, 4.9% MgO). A grain of Ca-rich plagioclase (about 1 mg, An<sub>95</sub>, FeO<sub>t</sub> = 0.4 wt.%) and 10 mg of powdered glasses were sealed in Au<sub>80</sub>Pd<sub>20</sub> alloy capsule, and then kept at around liquidus temperature. Liquidus phase of MTL rock at 350 MPa is always plagioclase with 0 to 5.5 wt.% H<sub>2</sub>O in melt (Ushioda, unpublished data), and therefore, a grain of plagioclase and hydrous melt are nearly in equilibrium. Oxygen fugacity (*f*O<sub>2</sub>) during the melting experiments was not controlled, and the intrinsic *f*O<sub>2</sub> of the pressure vessel was estimated to be 3 log unit above Ni-NiO buffer. Experiments were quenched after 24-48 hours, long enough to attain equilibrium partitioning of hydrogen between plagioclase and melt. Concentration of H<sub>2</sub>O in melt (both molecular H<sub>2</sub>O and OH) and concentration of OH in plagioclase was analyzed by infrared spectroscopy.

**Results:** Experimental results are summarized in Fig. 1. Correlation between total H<sub>2</sub>O (molecular H<sub>2</sub>O and OH) concentration in melt and OH concentration in plagioclase is non-linear: partition coefficient in molar basis is about 0.01 with low H<sub>2</sub>O in melt (< 1 wt.%), while it decreases with increasing H<sub>2</sub>O in melt (Fig. 1a). The OH concentration of plagioclase reaches 200-250 wt. ppm H<sub>2</sub>O with > 4 wt.% H<sub>2</sub>O in melt and saturates. OH in plagioclase linearly correlates with OH in melt (Fig. 1b), which confirms that hydrous species in plagioclase is OH ion as suggested by previous studies.

**Application:** The OH concentration of Ca-rich plagioclase (about An<sub>90</sub>) from the 1986 summit eruption of Izu-Oshima volcano, also a frontal-arc volcano in Izu-arc, shows variation ranging from <50 wt. ppm H<sub>2</sub>O through 300 wt. ppm H<sub>2</sub>O as a result of polybaric degassing (Hamada et al., 2011, EPSL). Hamada et al. (2011) claims that pre-eruptive melt dissolves H<sub>2</sub>O up to 6 wt.% and that melt undergoes polybaric degassing during ascent and eruption, based on (i) variation of OH in plagioclase, (ii) hydrous melting experiments to crystallize An<sub>90</sub> plagioclase, and (iii) geophysical observation of the 1986 summit eruption of Izu-Oshima volcano. In consistent with previous studies, this experimental studies demonstrates that plagioclase with >250 wt. ppm H<sub>2</sub>O can be in equilibrium with melt dissolving >4 wt.% H<sub>2</sub>O (Fig. 1a). Such high H<sub>2</sub>O concentration corresponds to saturated H<sub>2</sub>O concentration in melt at 8 to 10-km-deep magma chambers beneath Izu-Oshima volcano (Mikada et al., 1997, PEPI). Plagioclase from the 1986 summit eruption of Izu-Oshima volcano is expected to record polybaric degassing history of H<sub>2</sub>O-saturated magma during eruption.

Keywords: Water in nominally anhydrous minerals, plagioclase, arc basaltic magma, hydrous melting experiment

SCG65-P02

Room:Convention Hall

Time:May 20 17:15-18:30

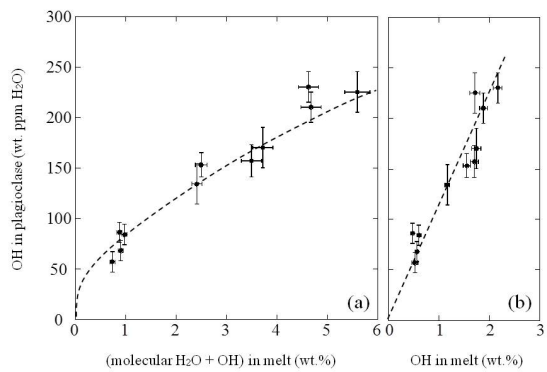


Fig. 1

## What stays in the slab and what returns to the surface? A geochemical mass balance model perspective

KIMURA, Jun-Ichi<sup>1\*</sup>, KAWABATA, Hiroshi<sup>1</sup>, Bladley Hacker<sup>2</sup>, Peter van Keken<sup>3</sup>, James Gill<sup>4</sup>, Robert Stern<sup>5</sup>

<sup>1</sup>IFREE/JAMSTEC, <sup>2</sup>University of California, Santa Barbara, <sup>3</sup>University of Michigan, <sup>4</sup>University of California Santa Cruz, <sup>5</sup>University of Texas at Dallas

We have developed the Arc Basalt Simulator (ABS), a quantitative forward model to calculate the mass balance of slab dehydration and melting, and slab fluid/melt-fluxed mantle melting, in order to quantitatively evaluate magma genesis beneath arcs. ABS models can reproduce magma compositions in many arcs.

The model suggests that the slab-derived component at volcanic fronts (VF) is mostly generated by dehydration, but successful models for most VF and all rear arc (RA) magmas also require the slab to melt. The compositions of slab fluids and melts are controlled primarily by the breakdown of amphibole and lawsonite beneath the VF and by the breakdown of phengite beneath the RA in addition to residual eclogite mineral phases including garnet, clinopyroxene, and quartz.

In the model, about 78-98% of relatively fluid-immobile elements including Nd and Hf in the arc lavas come from mantle peridotite. However, most liquid-mobile elements come from the slab. Modeled residual peridotite compositions are similar to those in some supra-subduction zone ophiolites and mantle xenoliths, providing constraints on reactions in the mantle wedge.

Altered oceanic crust (AOC) and sediment in the residual slab are modified by the subtraction of melt- and fluid-mobile elements. Unmodified AOC potentially becomes the EM I mantle component after 1 Ga, whereas melted AOC can have extremely fractionated U-Pb and become the HIMU source after 1-2 Ga. Element re-distribution beneath arcs can form the recycled materials that have been detected in ocean island basalts.

Keywords: arc, magma, geochemistry, mass balance

## Pb isotopic compositions of hydrothermal deposits in the Japanese island arc

FUJINAGA, Koichiro<sup>1\*</sup>, KATO, Yasuhiro<sup>1</sup>, HIEDA, Yuki<sup>1</sup>, TAKAYA, Yutaro<sup>1</sup>, Masaharu Tanimizu<sup>2</sup>, SHIMIZU, Toru<sup>4</sup>, NAKAMURA, Hitomi<sup>3</sup>, IWAMORI, Hikaru<sup>3</sup>

<sup>1</sup>University of Tokyo, <sup>2</sup>JAMSTEC, <sup>3</sup>Tokyo Institute of Technology, <sup>4</sup>Geological Survey of Japan

Quite recently, it has been pointed out that "geofluids" released from the subducting plates may be involved in various phenomena in subduction zone, such as young volcanic rocks, deep-seated hot springs and hydrothermal deposits. Systematical investigations of these various materials are needed for identifying the geochemical characteristics of the geofluids. Nakamura et al. (2008) revealed that the slab-fluids derived from two subducted plates (the Pacific plate and the Philippine Sea plate) contribute largely to the genesis of arc magmas in the Central Japan. Here we focus on hydrothermal deposits (vein-type and skarn-type) in the Japanese island arc. Hydrothermal fluids that formed sulphide mineral (galena, pyrite, chalcopyrite, sphalerite etc.) deposits are generally considered to have been derived from magmatic and/or meteoric waters based on H, C, O, and S isotopes in the deposit materials. However, ore fluids may be derived from deep slab-fluids. We report Pb isotopic compositions of hydrothermal deposits in the Japanese island arc and discuss about the origin of ore fluids.

Keywords: Pb isotopic composition, hydrothermal deposit, slab-fluid

## Rare earth element composition of the Arima-type brine and its implication for slab-derived fluid

YOSHIYUKI, Fujita<sup>1\*</sup>, NAKAMURA, Hitomi<sup>1</sup>, KUSUDA, Chiho<sup>2</sup>, IWAMORI, Hikaru<sup>1</sup>

<sup>1</sup>Department of Earth and Planetary Sciences, Tokyo Institute of Technology, <sup>2</sup>Department of Earth and Planetary Science, The University of Tokyo

The Arima-type brine has been known as one of the oldest hot springs in Japan, as well as its distinct geochemistry: in spite of its presence in the non-volcanic region in the forearc, the oxygen and hydrogen isotope compositions show a presence of deep brine similar to volcanic fluids. Mixing between the meteoric water and a deep brine with a high  $\delta^{18}\text{O}$  and  $\delta^2\text{H}$  (7 to 8, -40 to -30, respectively) explains the linear trend of the brine samples. The Arima-type brines are highly concentrated in the type locality, Arima, SW Japan. The two plates subduct beneath the area: the Pacific Plate subducts from the east and underlies ~400 km below the area, whereas the Philippine Sea Plate subducts from the southeast and is seismically observed 50 to 80 km below the area. In spite of this active subduction, there is no Quaternary volcano in this area, possibly because the Pacific Plate is too deep and the Philippine Sea Plate is too shallow to fulfill the physicochemical conditions for arc magma generation.

Here we report geochemical signatures, in particular the REE concentrations, of the Arima brine, and suggest that it could have originated directly from the subducting slab without any significant modification during its ascent. High salinity, high  $^3\text{He}/^4\text{He}$  ratio and distinct oxygen, hydrogen and carbon and strontium isotope compositions also suggest that they have been derived possibly from the subducting Philippine Sea slab, hence may bring invaluable insights for the slab-derived fluid and the related fluid processes in subduction zones. In this study, we analyzed samples from 'Kinsen'. The Kinsen brine has a high salinity and the highest abundances of the trace elements in this area. We have also sampled a solid material precipitated within the pipe, in order to estimate the elemental fractionation during cooling of the hot spring and precipitation from it. Because of its high salinity (up to 6 wt.% NaCl) of the Arima-type brine, the matrix effects are extremely large to prevent accurate analysis of any trace element. We employ a standard addition method, aiming at rapid yet accurate analyses.

The DMM normalized composition of Arima brine exhibits broadly a flat pattern around the normalized concentration of 10-3 with a convex-down shape for mid-REE, except for positive anomaly in Eu. On the other hand, the precipitates consist of aragonite and magnesite, which do not contain REE above the detection limit, except for Gd which is likely derived as flakes from the pipe.

Alternatively, based on the reported partition coefficient and the numerical modeling of the thermal structure along the subducting slab, the REE concentrations in the slab-derived fluid (as a product of slab dehydration reactions) have been evaluated. The calculation results broadly coincide with the observed REE concentrations of the Arima-type brine. Together with these analytical results and forward calculation, we conclude that the REE composition in the Arima brine is straightly originated from the dehydration of subducting slab at 450 degree.

Keywords: slab-derived fluid, Arima brine, rare earth elements, isotopic compositions of oxygen and hydrogen, Arima-type brine, subduction zone

## Two-stage serpentinization reactions: an example of Iwanai-dake ultramafic rocks, Kamuikotan belt, Hokkaido, Japan.

MIYOSHI, Akane<sup>1\*</sup>, KOGISO, Tetsu<sup>1</sup>

<sup>1</sup>Human and Environmental Studies, Kyoto University

The transformation of ultramafic rocks to serpentinites is an important process that influences geodynamic systems in subduction zones. Serpentinization changes physical properties of mantle peridotite. Furthermore, serpentinization in subduction zone affects water and material circulation and mantle dynamics. Despite this renewed interest in serpentinization, the underlying peridotite-water reactions are poorly understood. In recent years, a two stage model for serpentinization has been proposed. Serpentinization generally produces a large amount of magnetite, and petrography and magnetic properties of serpentinite show that magnetite is formed at the later stage of serpentinization. For example, Bach et al. (2006) proposed the formation of magnetite during the breakdown of brucite. On the other hand, Frost and Beard (2007) proposed the breakdown of ferroan serpentine under low silica activity condition. In addition to these, various reactions have been proposed. Although magnetite is an important factor that affects density or magnetic susceptibility of rocks, the previous studies didn't show enough petrographical evidence that support for the reactions proposed. In this study, serpentinization processes of Iwanai-dake peridotite, Kamuikotan belt, Hokkaido, have been investigated with petrological observations, chemical analyses, measurement of density and magnetic susceptibility. On the basis of these data, we discuss chemical processes that are responsible for magnetite formation.

The Iwanai-dake ultramafic body is located in the southern part of Kamuikotan belt, Hokkaido, Japan. A fresh peridotite body, which is about 1 km diameter, is located at the top of Mt. Iwanai-dake. It comprises harzburgite with a small amount of dunite. Ultramafic rocks surrounding peridotite are partly or completely serpentinized. Textures and mineral assemblages were identified by petrographic observation, and Raman spectroscopy. Mineral composition was determined by SEM-EDS. The serpentinite samples mainly consist of serpentine, brucite, and magnetite. Serpentine shows typical mesh textures. There are two kinds of mesh rim types in this area: Type A (Mg#97 serpentine and Mg#75 brucite) and, Type B (Mg#93 serpentine). Type B is associated with Mg#90 brucite vein in the central part. In harzburgite, with progress of serpentinization, mesh rim texture changes from Type A to Type A+B, and Type B only. Type B is always associated with serpentinization of orthopyroxene. Type B and Mg#90 brucite vein are not observed in dunite. The magnetic susceptibility of harzburgite increases rapidly with increasing amount of serpentine, but that of dunite remains low. It is shown that magnetite appear only high-serpentinized harzburgite.

These observations show that the serpentinization proceeded as follows: First, Mg#95-97 serpentine and Mg#75 Brucite were formed by isochemical reaction of olivine-H<sub>2</sub>O. Second, Mg#93 serpentine (and Mg#90 Brucite vein) was formed. The second stage reaction was caused by addition of SiO<sub>2</sub> rich fluid from serpentinization of orthopyroxene, as evidenced by no observation of the second stage reaction in dunite sample. Relation between magnetic susceptibility and density shows that magnetite was formed at the second-stage serpentinization. It is thought that the supply of SiO<sub>2</sub> was the trigger of the formation of magnetite. The result differs from the proposal of Frost and Beard (2007). However, the textural classification in this study is inapplicable to the texture discussed by Bach et al. (2006). It is necessary to consider that serpentinization depends on tectonic setting, chemical component of fluid, or mineral assemblage of protolith.

References: Bach, W., H. Paulick, C. J. Garrido, B. Ildefonse, W. P. Meurer, and S. E. Humphris (2006), *Geophys. Res. Lett.*, 33, L13306, doi:10.1029/2006GL025681. ; Frost, B. R. & Beard, J. S. (2007). On silica activity and serpentinization. *Journal of Petrology* 48, 1351-1368.



## Cl-bearing CO<sub>2</sub>-H<sub>2</sub>O fluid-inclusions of peridotite xenoliths from Ichinomegata

KUMAGAI, yoshitaka<sup>1\*</sup>, Tatsuhiko Kawamoto<sup>1</sup>, Junji Yamamoto<sup>1</sup>

<sup>1</sup>Inst. Geothermal Sci., Kyoto Univ.

Hydrous minerals in a subducting slab carry OH- and H<sub>2</sub>O into the Earth's interior, and at points beyond their stability conditions they release H<sub>2</sub>O to the overriding mantle wedge (Tatsumi and Eggins 1995). The H<sub>2</sub>O fluids transport materials from the slab to the mantle wedge. Recently, analyses of halogen elements of high-pressure metamorphic rocks suggest that saline fluids are preserved in the subducting slab as marine pore-fluids until the depths of at least 100 km (Sumino et al., 2010, EPSL). Salinity of H<sub>2</sub>O fluids affects dissolution properties of metal ions (Keppler, 1996, Nature). It is, therefore, important to understand the salinity of the H<sub>2</sub>O fluids in the mantle wedge in terms of subduction system of metal.

Fluid inclusions in mantle xenoliths preserve direct information of the fluids in the mantle. Mantle xenoliths from the Ichinomegata volcano, located in back-arc side in the northeast Japan arc, have CO<sub>2</sub>-H<sub>2</sub>O fluid inclusions (Roedder, 1965, Am Mineral). In the present study, we report salinity of the CO<sub>2</sub>-H<sub>2</sub>O fluid inclusions in the mantle xenoliths from the Ichinomegata volcano.

All mantle xenoliths studied are porphyroclastic lherzolite, composed of olivine, orthopyroxene, clinopyroxene, spinel and hornblende. The CO<sub>2</sub>-H<sub>2</sub>O fluid inclusions are occasionally present in orthopyroxene porphyroclasts. The fluid inclusions have not reacted with host orthopyroxene crystals after the formation. We suppose, therefore, that the salinity of the fluid inclusions represents the original value in the mantle. Formation depths of the fluid inclusions are estimated by the following steps: (1) estimating the bulk mole volume of CO<sub>2</sub>-H<sub>2</sub>O fluid inclusion using homogenization temperatures of CO<sub>2</sub> liquid-vapor and CO<sub>2</sub>-H<sub>2</sub>O (Bakker and Diamond, 2000, *Geochem. Cosmochim. Acta*), (2) calculating pressure of the formation of the fluid inclusion using equilibrium temperature estimated by a pyroxene geothermometer (Wells 1977, *Contrib.Mineral. Petrol.*) and isochore of CO<sub>2</sub>-H<sub>2</sub>O system (Loner AP, from Software Package FLUIDS, v.2, Bakker), (3) converting the pressure to depth by assuming densities of crust and mantle are 2.85 and 3.3 g/cm<sup>3</sup>, respectively, and Mohorovicic discontinuity is 27 km. Salinities of fluid inclusions are determined using melting temperature of clathrate (Darling, 1991, *Geochim. Cosmochim. Acta*). The depth is estimated to be about 30 km, which is consistent with the following petrographical feature. Some xenoliths have plagioclase and symplectites formed by reaction of plagioclase and olivine. This indicates that the xenoliths were from the boundary between plagioclase-peridotite and spinel-peridotite. The salinity of fluid inclusions is 3.93 ± 0.55 wt %. Using relationship between the molinity of Cl and the fluid/melt partition coefficients (Zajacz et al., 2008, *Geochem. Cosmochim. Acta*), for example, the fluid/melt partition coefficients of Pb and Zn under this salinity are 7.8 and 18.6, respectively (those of Cl-free hydrous fluid are almost 0 and 8.2, respectively).

Keywords: salinity, fluid inclusion, material transport, subduction zone, mantle xenolith, Ichinomegata



## Numerical simulations of temperature distributions associated with subduction of the plate beneath Tohoku and Kanto

TAKAGI, Rumi<sup>1\*</sup>, YOSHIOKA, Shoichi<sup>2</sup>, MATSUMOTO, Takumi<sup>3</sup>

<sup>1</sup>Dept. of Earth and Planetary Sci., Kobe Univ., <sup>2</sup>RCUSS, Kobe Univ., <sup>3</sup>Earthquake Research Department, NIED

### 1. Introduction

The Pacific plate is subducting beneath the Tohoku district, whereas the Philippine Sea plate is subducting beneath the Kanto district, overlapping on the top of the Pacific plate. In this study, firstly, we performed numerical simulations of temperature distribution associated with subduction of the Pacific plate beneath the Tohoku district. Secondly, based on the obtained temperature distribution beneath the Tohoku district, we performed numerical simulations of temperature distribution beneath the Kanto district, by incorporating subduction of the Philippine Sea plate.

### 2. Models and Methods

We calculated temperature distribution, using a 2-D box-type thermal convection model developed by Yoshioka and San-shadokoro (2002). We gave subduction velocity of the Pacific plate, referring to Sella et al. (2002). We changed the age of the subducting plate according to Sdrolias et al. (2006). Based on Nakajima et al. (2007, 2009) and Hirose et al. (2008), we gave the shape of the upper surface of the Pacific and the Philippine Sea plates. We used heat flow data of bore holes & heat probe (Tanaka et al., 2004; Yamano, 2004) and Hi-net in the wells (Matsumoto, 2007).

In the model of Takagi et al. (2011), mantle flow with high temperature took place near the tip of the mantle wedge associated with subduction of the Pacific plate beneath the Kanto district. This resulted in much higher calculated heat flow than observed one just above the tip of the mantle wedge with high temperature. Therefore, we constructed a domain where mantle flow does not flow into near the tip of the mantle wedge, which is referred to as the cold nose. Comparing observed heat flow data with those calculated from the temperature distribution obtained by numerical simulation beneath the Tohoku district, we constructed a temperature model which reproduces the observed heat flow values. We attempted to explain the observed low heat flow field spreading in the Kanto district, by subduction of the Philippine Sea plate in the model used for the Tohoku district.

### 3. Result

Incorporating the cold nose, we obtained a result which fits the observed heat flow values in the area of the oceanic side of the Tohoku district. In the Kanto district, the subduction of the Philippine Sea plate produced low heat flow region in the area of the landward side of the cold nose. To explain the observed heat flow values better in the Kanto district, we are also considering introducing frictional heating on the upper surface of the subducting Pacific plate.

Keywords: subduction, temperature distribution, flow field, heat flow, Kanto district, cold nose

## Three-dimensional electromagnetic imaging of NE Japan

OGAWA, Yasuo<sup>1\*</sup>, ICHIKI, Masahiro<sup>2</sup>, KANDA, Wataru<sup>1</sup>

<sup>1</sup>Volcanic Fluid Res. Centr., Tokyo Institute of Technology, <sup>2</sup>Tohoku University

Geofluid plays an important role in the genesis of crustal earthquakes and volcanoes. Magnetotelluric method uses natural electromagnetic fields and it can image the fluid distribution in terms of electrical resistivity. We have selected an area around Naruko volcano for our project target in order to get detailed three-dimensional distribution of fluids in the crust with a horizontal resolution of ~3km. From the analyses of previous data of 60 MT stations, we have found (1)sub-vertical conductors at the active volcanoes, like Naruko and Onikobe and (2)lower crustal conductors with SSW-NNE strike in the backarc side, and (3)upper to middle crustal conductors in the forearc. We have found high seismicity, located over or outside the crustal conductors.

In this presentation, newly obtained 81 MT data over the two large calderas, Mukaimachi caldera and Sanzugawa caldera, and three-dimensional modeling results will be presented.

Keywords: geofluid, electromagnetic exploration, resistivity, earthquake, volcano, caldera

## 3D seismic velocity structure around Philippine Sea slab subducting beneath Kii Peninsula

SHIBUTANI, Takuo<sup>1\*</sup>, FUKUI, Taishi<sup>2</sup>, HIRAHARA, Kazuro<sup>3</sup>, Setsuro Nakao<sup>1</sup>

<sup>1</sup>DPRI, Kyoto Univ, <sup>2</sup>NIDEC, <sup>3</sup>Science, Kyoto Univ

### 1. Introduction

Deep low frequency events (DLFEs) are distributed widely from western Shikoku to central Tokai (Obara, 2002; Kamaya and Katsumata, 2004; Obara and Hirose, 2006). Results from seismic tomographies and receiver function analyses revealed that the oceanic crust of the Philippine Sea plate has a low velocity and a high  $V_p/V_s$  ratio (Hirose et al., 2007; Ueno et al., 2008). Hot springs with high  $^3\text{He}/^4\text{He}$  ratios are found in an area between central Kinki and Kii Peninsula despite in the forearc region (Sano and Wakita, 1985; Wakita and Sano, 1987). These phenomena suggest the process that H<sub>2</sub>O subducting with the oceanic crust dehydrates at the depths of 30 - 40 km, causes the DLFEs, and uprises to shallower depths.

We carried out seismic observations in Kii Peninsula since 2004 in order to estimate the structure of the Philippine Sea plate and the surrounding area. We deployed seismometers along profile lines with an average spacing of ~ 5 km. We applied receiver function analyses and obtained images of S wave velocity discontinuities. In the previous presentation (Shibutani et al., 2010), we reported results for four profile lines in the NNW-SSE direction, that is the dip direction of the Philippine Sea plate and for a profile line in the NNW-SSE direction that is almost perpendicular to the dip direction. In this presentation we will report results of a seismic tomography in which we used information of seismic velocity discontinuities derived from the receiver function images and observed travel times at stations of the dense linear arrays.

### 2. Seismic travel time tomography

We implemented three dimensional geometry of the continental Moho, the upper surface of the oceanic crust and the oceanic Moho derived from the receiver function analyses to the velocity model. We used a fast marching method (de Kool et al., 2006) based on wavefront tracking for the theoretical travel time calculation. We also used observed travel times at temporary stations in the dense linear arrays in addition to permanent stations. A dense distribution of the temporary stations contributed to higher resolutions of tomographic images.

### 3. Structure around Philippine Sea slab

A result of the seismic tomography is shown in Fig.1. At the depth of 40 km the oceanic crust shows low velocity anomaly. As we go up to shallower depths, the low velocity anomaly seems to continue to the mantle wedge and to the lower crust. It becomes a large low velocity region at the depth of 16 km under the northwestern part of the Kii Peninsula. It is known that seismic activity is very high in the upper crust above the low velocity region. The low velocity anomaly is more significant in a western part of the Kii Peninsula.

We found differences also in the receiver function images between in the central to western part and in the eastern part. Beneath the former part, a low velocity region swells out into the mantle wedge from a dehydration area in the oceanic crust; the oceanic Moho becomes unclear below 40 km depth; the slab shows a convex upward bending shape. On the other hand, beneath the latter part, the oceanic Moho is uniformly clear down to 70 km depth; the slab shows a linear shape (Shibutani et al., 2010).

These features in the tomographic images and the receiver function images show that hydrous minerals in the oceanic crust are broken down by dehydration at the DLFE area, then the dehydrated fluids flow into the mantle wedge and the lower crust, and reduce the velocity in the regions. The differences in the structure and geometry of the slab and the mantle wedge between the central to western part and the eastern part of the peninsula can be explained by the amount of 'water' discharged into the mantle wedge and that left in the oceanic crust beneath 40 km depth through the dehydration.

We used waveform data from permanent stations of NIED; JMA; ERI, Univ. of Tokyo; Nagoya Univ. and DPRI, Kyoto Univ.

Keywords: tomography, receiver function, Philippine Sea slab, Kii Peninsula, slab-derived fluid

SCG65-P10

Room:Convention Hall

Time:May 20 17:15-18:30

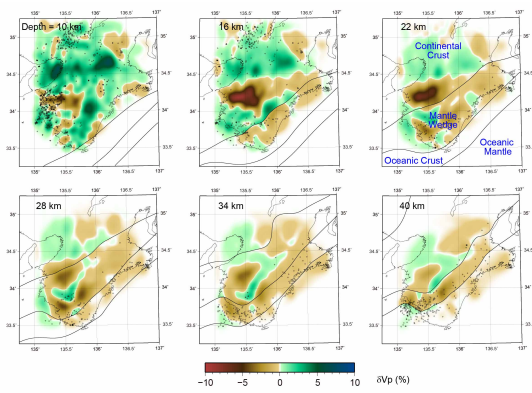


Figure 1 P wave velocity perturbation from an initial model at the depths of 10, 16, 22, 28, 34 and 40 km. The initial model is constructed basically on JMA2001 (Ueno et al., 2002) with a modification of -5 % velocity in the oceanic crust and +5 % velocity in the oceanic mantle and the mantle wedge. Circles indicate earthquakes which were used in the seismic tomography and occurred in the vicinity of each depth. The thick lines denote the continental Moho, the upper surface of the oceanic crust and the oceanic Moho from north to south.

## Li/B RATIO OF CRUSH-LEACHED FLUID OBTAINED FROM THE SANBAGAWA METAMORPHIC BELT: ITS AREAL DISTRIBUTION

HIRAJIMA, Takao<sup>1\*</sup>, Yoshida Kenta<sup>1</sup>, Sengen Yoshiteru<sup>1</sup>, Noguchi Naoki<sup>1</sup>, Kobayashi Tomoyuki<sup>2</sup>, MISHIMA Taketoshi<sup>2</sup>, Oh-sawa shinji<sup>2</sup>

<sup>1</sup>Graduate School of Science, Kyoto University,, <sup>2</sup>Institute for Geothermal Sciences, Graduate School of Sciences, Kyoto University

We investigated species and compositions of deep fluids trapped as fluid inclusions (FIs) in high-P met-amorphic rocks formed in the subduction zones. One of major goals of our deep fluid study is to testify an idea whether peculiar fluid soluble light elements, such as Li, B and Cl, can be used as an indicator of fluid generation depths in the subduction zones or not (Scambelluri et al. 2004).

Quantitative analyses of major and trace element composition of the deep fluid are still in the hard task. We adopted crush-leach (CL) technique (e.g., Banks and Yardley, 1992) for extracting FI from quartz veins/lenses developing parallel to the main foliation of Sanbagawa metamorphic rocks crystallized at 20 - 60 km depths.

Major cations/anions of CL fluids were analyzed by ion-chromatography, and Li and B were done by ICP-MS. Raman spectroscopy is adopted to determine the liquid and gas species of fluid inclusions in quartz. Microthermometry is adopted to estimate NaCl salinity and to identify the formation stage of FIs.

We extracted CL fluids from three areas of the Sanbagawa belt, 1) Wakayama area, 2) Asemigawa area and 3) Besshi area.

In Wakayama area, CL fluids were extracted from three samples of quartz veins hosted by metabasites covering the metamorphic grade from the chlorite zone, pumpellyite-actinolite facies equivalent, to the biotite zone, amphibolite facies equivalent. Their Li/B ratios increase with metamorphic grade of the host rocks from 0.02 to 0.10 (Sengen et al., 2009). The hydrochemical facies of CL fluids are X-HCO<sub>3</sub> type and the intermediate type between Na-Cl type and X-HCO<sub>3</sub> type. The texture of quartz grains, which retain FIs, show pervasively deformed and recrystallized type for all studied samples.

In Asemigawa area, CL fluids were extracted from six samples of quartz veins covering the metamorphic grade from the chlorite zone to the oligoclase-biotite zone. Their Li/B ratios mainly vary from 0.03 to 0.38, but there is no correlation between Li/B ratio and the metamorphic grade of host rocks. The hydrochemical facies of CL fluids are X-HCO<sub>3</sub> type, except for one sample of Na-Cl type. The texture of quartz grains show pervasively deformed and recrystallized type for all studied samples. Some host rocks show distinct S-C fabrics. These observations suggest the rocks in the Asemigawa area pervasively deformed during the exhumation stage.

In Besshi area, studied sample were collected from eclogite facies unit and neighboring schist units, equivalent with amphibolite facies. Li/B value of CL fluids varies from 0.10 to 1.99. Among all studied samples, relatively high Li/B (> 0.4 up to 2.0) ratio is identified only in this area. The samples with high Li/B ratio are characterized by both the Na-Cl type hydro-chemical facies and undeformed polygonal quartz fabric.

Two samples of quartz vein intercalated with eclogite show high Li/B ratio (0.27, 0.44), higher ratio of which is almost identical with those of dehydrated fluid from eclogite (Sengen et al., 2009; Marschall et al. 2007). Furthermore, CL fluids extracted from three samples of quartz veins intercalated with metasediments in the neighboring schist unit show much higher Li/B ratio (0.36-1.99). Yoshida et al. (2011) pointed out that Li/B ratio of dehydrated fluids was also controlled by the chemical composition of the host rock.

Raman spectroscopy and microthermometry clearly suggest that all samples applied CL technique contain fluids trapped at multi-stages, covering from prograde, peak and/or retrograde stages. However, some CL fluids obtained from quartz veins mostly free from post-peak deformation in the Besshi area have high Li/B ratio, which is almost identical with eclogite facies dehydrated fluids obtained from meta-serpentinite in Liguria and Betic Cordillera (Scambelluri et al. 2004). These facts suggest that Li/B ratio of dehydrated fluid has a potential for the indicator of the dehydration depth after considering some controlling factors.

Keywords: Deep fluid, Li, B, High-pressure metamorphic belt, Sanbagawa

## Fluid infiltration and change in mass transfer during the exhumation of Sanbagawa metamorphic belt, Japan

UNO, Masaoki<sup>1\*</sup>, IWAMORI, Hikaru<sup>1</sup>, NAKAMURA, Hitomi<sup>1</sup>, ISHIKAWA, Tsuyoshi<sup>2</sup>, Masaharu Tanimizu<sup>2</sup>, YOKOYAMA, Tetsuya<sup>1</sup>

<sup>1</sup>Department of Earth and Planetary Sciences, Tokyo Institute of Technology, <sup>2</sup>Kochi Institute for Core Sample Research, JAM-STE

**Introduction:** Individual parcel of regional metamorphic rock records physico-chemical conditions such as P-T path, mass transfer and deformation with the Lagrangian specification. On the other hand, a metamorphic belt as an ensemble of such parcels may provide a large-scale flow field of energy (e.g., temperature, entropy) and mass (including both solid and fluid phases with elements and isotopes) with the Eulerian specification. However, there are so far few models that integrate all the variables stated above. Phase petrology provides mostly the intensive variables (e.g., P-T path), whereas geochemistry provides mostly the extensive variables (time-integrated mass transfer), and these two have been treated separately. Here we combine phase petrology and geochemistry from a scale of mineral grain, and solve them under a simultaneous and consistent set of thermodynamic and mass balance equation. The results revealed the changes in mass transfer with changing P-T paths.

**Method:** The Sanbagawa metamorphic belt in Japan, the subduction-origin high-P type metamorphic belt, has been surveyed. To understand the nature of fluid during rehydration, we analyzed basic rocks that record retrograde reactions. Major and trace element compositions of each mineral, and bulk rock chemistry have been analyzed with EPMA, LA-ICP-MS, XRF and ICP-MS, respectively. Retrograde P-T path have been obtained by applying the Gibbs' method (e.g. Spear, 1993; Okamoto&Toriumi, 2001) to amphiboles and garnets.

Trace element budget along a specific P-T path were calculated by equating differential mass balance equation for major and trace elements as follows;

$$X_{fluid} dM_{fluid} = \text{Sum}(M_{solid} X_{solid}) + \text{Sum}(X_{solid} dM_{solid})$$

where  $X$  and  $M$  denote compositions and modes of minerals and  $dX$  and  $dM$  represent their changes along a specific P-T change.  $X_{solid}$ ,  $M_{solid}$ ,  $dM_{solid}$  for zoned minerals (amphibole and/or garnet) and  $X_{fluid}$  were derived from the results of Gibbs' method, X-ray map and fluid/mineral partition coefficients, respectively. Thus, the unknowns are  $dM$ s, and the equations are solved for them. As a result, the mass transfer during a specific P-T change ( $X_{fluid} dM_{fluid}$ ) can be specified.

Furthermore, trace element budget during rehydration reactions were also constrained based on proportionality of bulk fluid-mobile element composition with H<sub>2</sub>O (LOI (loss on ignition)). Based on a simple model that accounts for heterogeneity of protolith composition and devolatilization by dehydration reaction, the fluid composition during rehydration was estimated.

**Results and Discussion:** The P-T path obtained from the least rehydrated sample records the P-T path from 15kbar, 550°C to 11kbar 600°C, which corresponds to the exhumation just after the peak pressure condition. The mass balance analysis revealed that it was a dehydration reaction and Y and Cs increased whereas Ba decreased during this P-T path. No significant change was observed for Rb, Pb and Sr.

It is revealed that fluid mobile elements such as LIL elements, Sr and Pb are mostly proportional to LOI (loss on ignition). LOI and extent of rehydration are proportional in the Sanbagawa belt (Okamoto&Toriumi, 2005), thus the observed enrichment of LILE and Pb are interpreted to be associated with rehydration (from 11kbar 600°C to 3kbar 400°C). The Sr isotope ratios of the basic shists also increase with LOI, implying that the differences in bulk rock chemistry are due to an addition and/or reaction with external source of fluids with high <sup>87</sup>Sr/<sup>86</sup>Sr. The estimated fluid composition is similar to calculated compositions of slab-derived fluids (Nakamura et al., 2008).

Comparing the results of (1) the mass balance analysis with early part of exhumation P-T path and (2) bulk composition analysis reveals that the mode of mass transfer changed from Y and Cs enrichment with Ba depletion, to LILE (Li, K, Rb, Cs, Sr, Ba) and Pb enrichment, associated with the change in P-T path.

Keywords: fluid, mass transfer, metamorphism, subduction zone, Sanbagawa metamorphic belt, trace element



## Isotope and Boron of Quaternary lava in Central Sunda arc, Indonesia: an assessment of slab influence to mantle wedge

Haryo Edi Wibowo<sup>1\*</sup>, HASENAKA, Toshiaki<sup>1</sup>, HANDINI, Esti<sup>1</sup>, SHIBATA, Tomoyuki<sup>2</sup>, Yasushi Mori<sup>3</sup>, HARIJOKO, Agung<sup>4</sup>

<sup>1</sup>Department of Earth Science, Graduate School of Science and Technology, Kumamoto University, <sup>2</sup>Beppu Geothermal Research Laboratory, Kyoto University, <sup>3</sup>Kitakyushu Museum of Natural History and Human History, <sup>4</sup>Department of Geological Engineering, Gadjah Mada University

We estimated contribution of slab-derived fluid of the arc mantle beneath Central Sunda Arc (CSA) in order to better understand the subduction processes. Sunda arc, a part of Pacific ring of fire, extends from Sumatera to Flores. Magmatism beneath Sunda arc is associated with subduction process. CSA is represented by a series of Quaternary volcanoes from fore arc toward back arc, consisting of Merapi, Merbabu, Telomoyo, Ungaran and Muria. We analyzed samples from these volcanoes by using X-Ray Fluorescence, Prompt Gamma-Ray and Instrumental Neutron Activation Analysis. Representative samples were also analyzed by Thermal Ionization Mass Spectrometer to obtain  $^{87}\text{Sr}/^{86}\text{Sr}$  and  $^{143}\text{Nd}/^{144}\text{Nd}$  ratios.

Boron is distinctively enriched in ocean floor sediment and altered oceanic crust (AOC). Higher mobility of boron from sediment to sediment-derived fluid than that of altered oceanic crust makes distinction of fluid sources. Fluid contribution to source mantle was estimated by applying ratio of boron and other mobile elements against HFSE. Estimation at CSA shows general decreasing trend of fluid contribution toward back arc with the highest contribution observed in the middle (Telomoyo) of arc transect, instead of the volcanic front (Merapi). This pattern is different from that estimated by Sr-Nd isotope ratios which are sensitive to modification of mantle by sediment-derived fluid. These isotope ratios show that influence of slab smoothly decreases from volcanic front toward back arc. Distinction between contributions from sediment-derived fluid and AOC-derived fluid was generated by plots of B/La, Rb/La, B/Nb, Rb/Nb against those of Sr and Nd isotope ratios. These plots show that the highest contributions of sediment occur at the volcanic front, whereas that from AOC occurs just a little behind the volcanic front. In addition to the variability of slab-derived fluid contribution, the small variation in isotopic and Nb/Zr, Nb/Ta ratios among fore arc volcanoes of CSA indicate little heterogeneity of the mantle source beneath them. Exception comes from the back arc volcano, Muria, which indicates relatively enriched mantle with only a little slab influence.

Keywords: Boron, Subduction, Slab fluid, Sunda arc



## Development of A Preliminary Reference Rock Model for Physical Properties of Fluid-bearing Rocks

NAKAMURA, Michihiko<sup>1\*</sup>, WATANABE, Tohru<sup>2</sup>, IWAMORI, Hikaru<sup>3</sup>

<sup>1</sup>Department of Earth Science, Graduate School of Science, Tohoku University, <sup>2</sup>Graduate School of Science and Engineering, University of Toyama, <sup>3</sup>Department of Earth and Planetary Sciences, Tokyo Institute of Technology

**Backgrounds:** Recent advances in seismic tomography and magneto-telluric (MT) imaging have increased the potential for mapping the distribution of geological fluids (i.e., aqueous fluids and silicate melts) in the Earth's crust and uppermost mantle, since seismic velocity is sensitive to the fluid fraction, while electrical conductivity is strongly dependent on the connectivity of conductive fluid phases. To interpret the observed physical properties into the nature of the fluid, their correlation with the microstructure of fluid-bearing rocks is essential.

**Sources of uncertainty:** The seismic wave velocities are dependent on temperature and lithology, i.e., the phase and solid-solution compositions of the major minerals composing the rocks, besides on the fluid fraction. Especially in the middle and lower continental crusts, there is often considerable uncertainty regarding the lithology and temperature. Therefore, when the lithological and thermal structures are not well constrained, the uncertainties of the estimation of fluid distribution becomes large. On the other hand, the electrical conductivity is less dependent on the mineral compositions and phases, compared to the large contrast between those of silicate minerals and fluid phases. Although experimental data of electrical conductivity of minerals and fluids at elevated pressure and temperature are still insufficient, MT observations provide important constrains on the fluid distribution in the crust and mantle.

**Scale resolutions of the geophysical imaging and length scale of geological heterogeneity:** The observed seismic velocity is an average value typically in a km scale. Space resolution of the MT imaging is a few to tens of km, dependent on the depth. Given the high electrical conductivity in the middle to lower crusts of active convergent margins, interconnection of the fluid phases should be established in these km scales.

**Role of heterogeneity:** Since the dihedral angles between aqueous fluids and minerals in crustal conditions are generally larger than 60 degree, large fluid fraction is required for the fluid interconnection. The saline components in the fluids decrease the dihedral angle, but carbon dioxide increases, counteracting with each other. The veins and cracks can increase the fluid connectivity locally and anisotropically, but their individual length scale is much smaller than the imaging resolution. There are several other mechanisms to produce small scale heterogeneity or fabrics of the fluid distribution, but they may not responsible for the pervasive fluid interconnection in a km scale. Therefore, grain-scale fluid interconnection is still the first hypothesis to be tested. The relation between the volume fraction and connectivity of the pore fluids should be quantitatively understood for major crustal rocks.

**The PROM project:** In this context, we have reviewed and compiled the data of seismic velocities, electrical conductivities, and dihedral angles and other microstructural factors that determine the grain-scale fluid distribution for the rocks of crust and uppermost mantle. Although lack of the physical property data at elevated pressure and temperatures does not allow us to develop a comprehensive data base, a possible data set composed of some major rock types and their physical properties as a function of fluid fraction can be presented as a preliminary reference model for the crustal rocks.

**Keywords:** physical property of rocks, pore fluid, microstructure

## Shear wave polarization anisotropy induced by C-type olivine LPO and fluid distribution beneath southern Kyushu

TERADA, Tadashi<sup>1</sup>, HIRAMATSU, Yoshihiro<sup>1\*</sup>, MIZUKAMI, Tomoyuki<sup>1</sup>

<sup>1</sup>Department of Earth Sciences, Kanazawa University

A high  $V_p/V_s$  region detected by seismic tomography suggests the existence of fluid and serpentinized peridotite near the slab surface beneath the southern Kyushu region, Japan (Matsubara and Obara, 2011). The existence of fluid and serpentinite plays an important role for volcanism and seismicity in subduction zones. The distribution of fluid and serpentinite are, therefore, significant for considering the dynamics of subduction zones.

In this study, we perform the shear wave splitting analysis to detect the seismic anisotropy near the slab surface beneath the southern Kyushu region using shear wave splitting. In this study, we compare observations with theoretical values calculated from mineral elastic constants, discuss the cause of seismic anisotropy and infer the distribution of fluid and serpentinite beneath the southern Kyushu region.

We use events, whose source depth is greater than 30 km and magnitude is greater than 2.5, from 2004 to 2010 recorded at Hi-net stations in the southern Kyushu region. The observed polarization direction and delay time are NEE-SWW to NWW-SEE and 0.04-0.63 s, respectively. Previous works showed that the delay time is less than 0.3 s for shear wave splitting induced by the crustal anisotropy. The observed shear wave splitting whose time delay is greater than 0.3 s, therefore, originates from the seismic anisotropy in the mantle.

In the southern Kyushu region, a lot of split shear waves whose delay time is greater than 0.3 s pass through the high  $V_p/V_s$  region at the depth of 100-150 km. From the comparison of other ray paths, seismic anisotropy can be restricted in this region. The theoretical calculation shows that the Lattice Preferred Orientation (LPO) of C-type olivine fabric with the trench parallel b-axis and the trench normal c-axis inclined 60 degrees from the horizontal can reproduce the observations. We, therefore, suggest that C-type olivine fabric LPO causes the seismic anisotropy beneath the southern Kyushu and the thickness of the anisotropic layer is estimated to be about 13-30 km. This result suggests also that the existence of fluid in this region. We, thus, consider that the migration of interstitial fluid in peridotite is activated due to a decrease of the dihedral angle of olivine fluid interface (Mibe et al., 1999) at the depth below 100 km beneath the southern Kyushu region.

In this study, we observe no shear wave splitting induced by serpentine in the forearc mantle wedge. This result does not contradict the existence of a thin serpentine layer (1~3 km) proposed by Hilairet and Reynard (2009).

Keywords: shear wave polarization anisotropy, C-type olivine, LPO, fluid, serpentine

## SYNTHETIC EXPERIMENTS OF AQUEOUS AND CARBONATE FLUID INCLUSIONS

OHI, Shugo<sup>1\*</sup>, Tetsu Kogiso<sup>1</sup>, Takao Hirajima<sup>2</sup>

<sup>1</sup>Human and Environmental studies, Kyoto University, <sup>2</sup>Science, Kyoto University

Deep aqueous fluids from subducted slab affect volcanic activity and seismicity in the subduction zone. (e.g., Schmidt and Poli, 1998) To reveal the chemistry of slab-derived fluids is crucial for understanding the material circulation in subduction zones, but as yet it is very difficult to experimentally constrain the chemical composition of these fluids. Diamond-trap experiments in combination with LA-ICP-MS analyses of frozen samples have been used to analyze chemical compositions of aqueous fluids in equilibrium with complex mineral assemblages (e.g., Kessel et al., 2004). However, in order to accurately determine fluid compositions experiments also need to be designed to account for modification of the fluid during quenching. Synthetic fluid inclusions trapped during high-pressure experiments can keep the composition of the fluids produced at run conditions. We have developed a method to trap fluids liberated during decomposition of hydrous and carbonate minerals as fluid inclusions in a quartz crystal.

The synthetic fluid inclusion technique (Sterner and Bodnar, 1984) was employed in this study. Synthetic fluid inclusions were formed in synthetic quartz provided by Nihon Dempa Kogyo Co., LTD. Quartz single crystals were cut into about 1-2mm size, heated to 450 C, and then quenched in cold distilled water to make cracks within it. After drying in a vacuum oven at 150 C overnight, the quartz crystals with cracks were rapped in a piece of Pt foil (2.5um-thick) and sealed in Au or Pt capsules with various mineral assemblages, such as Mg(OH)<sub>2</sub>, CaCO<sub>3</sub>+SiO<sub>2</sub>, CaCO<sub>3</sub>+SiO<sub>2</sub>+H<sub>2</sub>O and mMgCO<sub>3</sub>Mg(OH)<sub>2</sub>nH<sub>2</sub>O+SiO<sub>2</sub>+Mg(OH)<sub>2</sub>. The capsule was placed in a solid-media piston-cylinder apparatus and kept at the pressure range 0.5-1 GPa and at the temperature range 800-1100 C for 3-192 hours.

After quenching, thin sections (200-500um-thick) were prepared to examine with an optical microscope, Raman spectroscopy and microthermometry. The analyses for microthermometry were performed by referring Diamond (2001) and using the computer program Loner AP (e.g., Bakker, 2009).

Fluids liberated from Mg(OH)<sub>2</sub> were successfully trapped as fluid inclusions in all experiments. Microthermometry for a fluid inclusion in the sample synthesized at 800 C and 1 GPa for 3 hours showed the homogenization temperature of 251 C, molar volume of 22.8 cm<sup>3</sup>/mol. However, the calculated isochore shows that the temperature calculated for 1 GPa was 961 C, which was different from the run condition.

Fluid inclusions were not observed in experiments with CaCO<sub>3</sub>+SiO<sub>2</sub>, whereas were successfully synthesized in experiments with CaCO<sub>3</sub>+SiO<sub>2</sub>+H<sub>2</sub>O. The size and amount of fluid inclusions in these samples were smaller than those in the experiments with Mg(OH)<sub>2</sub>. Raman spectra showed the peaks of CO<sub>2</sub> but the broad peaks of H<sub>2</sub>O were not observed clearly.

Fluids liberated from mMgCO<sub>3</sub>Mg(OH)<sub>2</sub>nH<sub>2</sub>O+SiO<sub>2</sub>+ Mg(OH)<sub>2</sub> were successfully trapped as fluid inclusions in all experiments. Raman spectra showed that the fluid inclusions in these samples were composed of H<sub>2</sub>O and CO<sub>2</sub>. Microthermometry for the three fluid inclusions in the sample synthesized at 850 C and 1GPa for 18 hours showed that the homogenization temperatures from vapor-liquid carbon phase to liquid carbon phase were 24-29.5 C and total homogenization temperatures were 255-269 C, yielding molar volumes of 24.2-26.3 cm<sup>3</sup>/mol and total mole fractions CO<sub>2</sub> of 12-18 mol%. The calculated isochores give 910-1033 C at 1GPa, which had wide distribution.

In the experiments of anhydrous systems, liberated fluid could not be trapped during crack healing or perhaps crack healing did not occur in the experimental conditions in present study. The temperatures estimated from microthermometry were different from run conditions.

To interpret the condition that fluid inclusions are produced, it is needed to figure out the reason of this discrepancy by more analyses with precise observations of occurrence.

Keywords: synthetic fluid inclusion, hydrous mineral, carbonate mineral, piston-cylinder

## Measurement of seismic velocity of crustal rocks under high confining pressure and pore pressure

HARADA, Yuya<sup>1\*</sup>, KATAYAMA, Ikuo<sup>2</sup>

<sup>1</sup>Department of Earth and Planetary Systems Science, Hiroshima University, <sup>2</sup>Department of Earth and Planetary Systems Science, Hiroshima University

### Introduction

Water of the earth interior is mainly supplied at the subduction zone and has important role on seismic activity and volcanism in island arc. It is guessed that slow slip events and tremors occurring at this region are related to water. Based on the seismic tomography at Kanto district, high Poisson's ratio area ( $\sim 0.337$ ) was observed and suggested weak seismic coupling (Kamiya and Kobayashi., 2000). Similar high Poisson's ratio is detected at Tonankai and Sikoku district, exceeding 0.3. Those regions correspond to the plate boundary generating slow slip events or tremors (Kodaira et al., 2004 ; Shelly et al., 2006). Because relatively young oceanic plates are subducting in districts from Kanto to Shikoku, antigorite which Poisson's ratio is  $\sim 0.29$  may exist stably in those areas. In this case, the observed high Poisson's ratio requires excess pore fluids in addition to the serpentinized mantle. In order to clarify geometry and the abundance of water, we investigate seismic velocity of crustal rocks under high confining pressure and pore fluid pressure.

### Experimental methods

For the measurement of seismic velocity, we used the hydraulic pressure vessel in Hiroshima University, in which seismic wave velocity was calculated by using pulse echo method. Samples are gabbro (from Belfast) and granite (from Inada) and were prepared into a cylindrical shape, which diameter and length is 20 and 5-10 mm. We measured seismic velocity under dry and wet conditions, in the later case, distilled water is supplied into the sample with pore pressure up to 50 MPa.

### Results and discussion

Under dry experiments, seismic velocities of gabbro and granite were measured up to confining pressure as high as 200MPa. Calculated seismic velocities of gabbro in each confining pressure (100, 140, and 180MPa) were  $V_p = 6.88, 6.94, 6.83$  km/s,  $V_s = 3.85, 3.91, 3.79$  km/s, and velocities of granite were ranging  $V_p = 4.94-6.09$  km/s and  $V_s = 2.89-3.36$  km/s under confining pressure of 200 MPa. These values are lower than Christensen (1996)'s experiments, but  $V_s$  of gabbro are similar to those values. From the measurement of both compression and decompression process, it is confirmed that velocity variation has the reproducibility and there is an effect depending on cracks or pores closed by high confining pressure.

Under wet experiments, granite was measured at confining pressure of 60 MPa with pore pressure of 50 MPa (effecting pressure of 10 MPa). At confining pressure of 60 MPa before raising pore pressure, velocities were  $V_p = 5.17-5.60$  km/s and  $V_s = 2.84-4.36$  km/s. After pore pressure increased to 50MPa, velocities were slightly changed to  $V_p = 5.02-5.18$  km/s,  $V_s = 2.13-3.64$  km/s. However, signal from the sample reflection is very weak and therefore these values have large uncertainty at this moment. It is likely that this pulse weakening is related to the wave splitting, overlapping with background noises, and the reflectivity between the sample and the spacer of sample assembly. We try to fix these issues and hope to present the effect of pore pressure on seismic velocity in the coming JPGU meeting.

Keywords: seismic velocity, crustal rock, Poisson's ratio, geofluid, pore pressure, subduction zone

## A three-dimensional electrical conductivity distribution model of the upper mantle beneath Tohoku district

ICHIKI, Masahiro<sup>1\*</sup>, OGAWA, Yasuo<sup>2</sup>, Songkhun Boonchaisuk<sup>2</sup>, DEMACHI, Tomotsugu<sup>1</sup>, FUKINO, Hiromi<sup>4</sup>, HIRAHARA, Satoshi<sup>1</sup>, HONKURA, Yoshimori<sup>2</sup>, KAIDA, Toshiki<sup>1</sup>, KANDA, Wataru<sup>2</sup>, KONO, Toshio<sup>1</sup>, KOYAMA, Takao<sup>3</sup>, MATSUSHIMA, Masaki<sup>4</sup>, NAKAYAMA, Takashi<sup>1</sup>, SUZUKI, Syuichi<sup>1</sup>, TOH, Hiroaki<sup>5</sup>, UYESHIMA, Makoto<sup>3</sup>

<sup>1</sup>Grad. Sch. of Sci., Tohoku Univ., <sup>2</sup>Volcanic Fluid Res. Center, Tokyo Tech, <sup>3</sup>Earthq. Res. Inst., Univ. Tokyo, <sup>4</sup>Grad. Sch. of Sci. and Eng., Tokyo Tech, <sup>5</sup>Grad. Sch. of Sci., Kyoto Univ.

While plenty of three-dimensional (3-D) seismic tomographic images has been revealed (e.g. Zhao et al., 1992; Nakajima et al., 2001), only a few 3-D electrical conductivity distribution model has been proposed in terms of wedge mantle in subduction zones (e.g. Patro et al., 2007). Introducing the state-of-the-art mobile magnetotelluric (MT) observation systems (LEMI-417 and NIMS), we have acquired MT data at Tohoku district, northeastern Japan for the aim of 3-D electrical conductivity distribution in the wedge mantle. Typical observation duration are three months at each site, and MT response functions from 10 to 20000 seconds in period have successfully collected with fine quality. The site location is arranged with ca. 20 km interval. The MT phase response functions at many sites show over 90 degrees over 5000 seconds and suggest that 3-D distribution beneath this area.

Simple checker board resolution tests have been performed to estimate resolution. Regular cubes with 40 km on side and 10 ohm-m in conductivity embedded in 1000 ohm-m matrix were clearly recovered down to 120 km in depth using the synthetic data, while those with 20 km on side were not recovered clearly.

We carried out the three-dimensional inversion analysis with WSINV3DMT code (Siripuvaporn et al., 2005). Although the inversion process is still on the way and the conversion is not enough, the east-west profile (across the Japan Arc) of the preliminary result shows that conductive region appears at about 120 km in depth beneath back-arc region and elongates obliquely towards the volcanic front. The north-south profile (along the Japan Arc) shows the vertical conductive and resistive columns appears alternatively. That basic images are well consisted with the seismic tomographic model (Nakajima et al., 2001), provided that conductive and low velocity zone should corresponds with each other. Obtained the final 3-D model, our final destination is to estimate the mantle geotherm and fluid distributions in the wedge mantle using seismic tomographic and electrical conductivity images.

## Numerical analyses of water content and melting regimes in the NE Japan arc

HORIUCHI, Shyunsuke<sup>1\*</sup>, Iwamori Hikaru<sup>2</sup>

<sup>1</sup>Earthquake Research Institute, The University of Tokyo, <sup>2</sup>Tokyo Institute of Technology

Melting and seismic structure beneath the northeast Japan arc considering upon the uncertainties of H<sub>2</sub>O content is modeled to estimate the relation between melting region and H<sub>2</sub>O content, and restrict water content distributed in mantle wedge. This model results show that increasing water content, a weak melting starts to occur beyond  $C_{H_2O} = 0.07$  wt%, and the calculated P-wave and S-wave velocity structures between  $C_{H_2O} = 0.10$  wt% and 0.40 wt% can explain tomographic low velocity zones. The distribution of melt production rate ( $C_{H_2O} = 0.15$  wt%) shows that all three mechanism (Flux, decompression, and compression melting) are necessary to explain volcanic activity at back arc, volcanic front, and intermediate region in the Northeast Japan arc. In the case of  $C_{H_2O} = 0.15$ -0.34 wt%, the model results of volcanic eruption rate can explain observed across-arc features in terms of relative intensities (i.e., spatial location and pattern). Considering into the comparison with tomographic data, melting mechanism, and the comparison with volcanic eruption data, this model results for  $C_{H_2O} = 0.15$ -0.34 wt% can explain volcanic activity in the Northeast Japan arc.

Keywords: water, melting, subduction zone